Journal of Power Sources 195 (2010) 3841–3848

Contents lists available at ScienceDirect

Journal of Power Sources

journal homepage: www.elsevier.com/locate/jpowsour

Synergistic enhancement of supercapacitance upon integration of nickel (II) octa [(3,5-biscarboxylate)-phenoxy] phthalocyanine with SWCNT-phenylamine

Bolade O. Agboola, Kenneth I. Ozoemena*

Energy and Processes, Materials Science and Manufacturing, Council for Scientific and Industrial Research (CSIR), Pretoria 0001, South Africa

ARTICLE INFO

Article history:
Received 1 October 2009
Received in revised form
18 November 2009
Accepted 20 December 2009
Available online 13 January 2010

Keywords:
Supercapacitance
Specific capacitance
Nickel (II) octa [(3
5-biscarboxylate)-phenoxy]
phthalocyanine (NiOBCPPc)
GCE-NiOBCPPc-SWCNT-phenylamine
hybrid

ABSTRACT

Supercapacitive behaviour of a novel functional material, nickel (II) octa [(3,5-biscarboxylate)-phenoxy] phthalocyanine (NiOBCPPc) upon covalent integration with phenylamine functionalized single-walled carbon nanotubes (SWCNT-phenylamine) is reported for the first time. The supercapacitive behaviour of the hybrid (NiOBCPPc-SWCNT-phenylamine) was investigated using galvanostatic charge–discharge and electrochemical impedance spectroscopy. Using a more reliable galvanostatic charge–discharge method, the NiOBCPPc-SWCNT-phenylamine hybrid exhibited superior geometrical capacitance (~186 mF cm^{-2}) compared to either NiOBCPPc (~54 mF cm^{-2}) or SWCNT-phenylamine (~74 mF cm^{-2}) at a current density of 138 μA cm^{-2}. The NiOBCPPc-SWCNT-phenylamine gave excellent stability of over 1000 charge–discharge continuous cycling.

1. Introduction

There is a considerable interest in the development of alternative energy storage/conversion devices with high power and energy densities in order to cater for the present day demands for energy in this ever growing world population and industrialization. In this respect, electrochemical capacitors or supercapacitors have been shown to be highly promising owing to their higher power density and durable longer cycle life compared to secondary batteries [1–5] and have shown great promising as suitable filling gap/replacements for batteries and normal capacitance [1–5] owing to their high specific power than batteries [1–9] and significantly higher capacitance (~10^5) than the normal capacitance [6–9]. SCs are broadly classified into two categories, electrical double-layer capacitors (EDLCs) and pseudocapacitors. The operation mechanism of the former involves the non-Faradaic separation of charges at the "double-layer" (i.e., electrode/electrolyte interface) while the latter involves fast Faradaic, redox reaction of electroactive materials at the interface.

Carbon nanotubes (CNTs) show interesting physico–chemical properties such as unique optical property, good electrical conductivity and high mechanical strength [10,11], and exhibit excellent electrocatalytic properties [12–19]. CNTs applications have included materials for secondary batteries [20,21] and supercapacitors [22–29]. Combination of CNTs with materials such as polypyrrole [28] and metal oxides [29] were shown to improve these materials supercapacitive behaviour. The thermal stability, porosity and high surface area of the CNTs make them as suitable materials for supercapacitors. Functionalization of CNTs, especially by chemical bonding with other interesting materials has attracted enormous interest recently [30–35]. The integration of CNTs with metallophthalocyanine (MPc) complexes has begun to attract some attention as such CNT-MPc hybrids can serve as efficient means of tuning the chemical and physical properties of MPc or CNTs towards specific applications as in electrocatalysis and sensing [15]. MPc complexes are well known to have interesting physico–chemical properties which make them very suitable to many applications in various fields such as photocopying and laser printing, electrochromic and electroluminescent display devices, optical computer re-writable compact discs and information storage systems, liquid crystal display devices, photovoltaic cells, fuel cells [36,37], and electrochemical sensors [38–42] just to mention but a few. Recently, we reported a new type MPc-CNT system, cobalt (II) octa [(3,5-biscarboxylate)-phenoxy] phthalocyanine (CoOBCPPc) integrated with phenylamine-functionalized single-walled carbon nanotubes (SWCNT-phenylamine) [43]. This novel CoOBCPPc-SWCNT-phenylamine hybrid showed good electrocatalytic properties towards the detection of an important

* Corresponding author. Tel.: +27 12 841 3664; fax: +27 12 841 2135.
E-mail address: kozoemena@csir.co.za (K.I. Ozoemena).

0378-7753/$ – see front matter © 2010 Elsevier B.V. All rights reserved.
doi:10.1016/j.jpowsour.2009.12.095

biological analyte, β-nicotinamide adenine dinucleotide (NADH) [43]. Indeed, this initial study has opened a wide window of research for this type of MPc-CNT system, especially considering that MPc complexes with different metal centres and/or substituents give different physico–chemical properties and potential applications.

The use of MPc-CNT system in supercapacitor development has recently been reported [44]. In this study, we report for the first time, the supercapacitive behaviour of a novel nickel (II) octa [(3,5-biscarboxylate)-phenoxy] phthalocyanine (NiOBCPPc) integrated with SWCNT-phenylamine. We reveal that these two π-electron species (NiOBCPPc and SWCNT-phenylamine) could synergistically enhance the supercapacitance when integrated to form the NiOBCPPc-SWCNT-phenylamine hybrid. The choice of the nickel-centred MPc complex for this study is motivated by the well known supercapacitive properties of nickel-based complexes [44,45].

2. Experimental

2.1. Materials and reagents

Single-walled carbon nanotubes (SWCNTs) were obtained from Aldrich and were functionalized with phenylamine using established methods [46]. All other materials and reagents such as *N,N′*-dicyclohexylcarbodiimide (DCC) and sodium sulphate were of analytical grade and were used as received from the suppliers without further purification. Ultra pure water of resistivity 18.2 MΩ cm was obtained from a Milli-Q Water System (Millipore Corp. Bedford, MA, USA) and was used throughout for the preparation of solutions.

2.1.1. Preparation of NiOBCPPc-SWCNT-phenylamine

First, the NiOBCPPc was synthesized using the established procedure reported in literature [43,47] (Scheme 1).

Briefly, a mixture of 4,5-dichlorophthalonitrile and 5-hydroxyisophthalate (1: 4 mol ratio) in 100 ml DMF under stirring at 65 °C for 24 h, and then an excess of K_2CO_3 is added at regular interval in the first 12 h of the reaction. A dinitrile product was obtained by careful extraction with chloroform, and crystallization from methanol. The pure dinitrile (800 mg) was mixed with 149.3 mg of nickel acetate, $Ni(OAc)_2{\cdot}2H_2O$ in *n*-pentanol (20 mL) with few drops of DBU and then heated for 12 h at 140 °C. Upon cooling, a crude greenish product was obtained, and purified by chromatography using a mixture of THF, dichloromethane and ethyl acetate (8:1:1) for elution. The product (an "ester product") was then converted to the final product by first reacting with saturated NaOH solution, water and methanol mixture, dried and finally treated with 1 M HCl until the solution reached pH 2. The resulting blue–green product was filtered and thoroughly washed with water to obtain the NiOBCPPc. Yield: 64%, Anal. Calcd. for $C_{96}H_{48}N_8O_{40}Co{\cdot}28H_2O$: C 45.59, H 3.83, N 4.92; Found: C 45.80, H 4.14, N 4.45. ESI-FTICR mass spectra analysis: *m*/*z* theoretical and actual (in bracket) values for species $(M\text{-}2H)^{2-}$, $(M\text{-}3H)^{3-}$, $(M\text{-}4H)^{4-}$ and $(M\text{-}5H)^{5-}$ are 1004.35 (1004.0573), 669.23 (669.0371), 501.68 (501.5260) and 401.14 (401.0193), respectively. UV–vis (DMF), λ_{max}(nm) ($\log\varepsilon$) in DMF: Q-band monomeric at 667 (4.70), Q-band aggregated at 621 (4.27), B-band at 286 (3.97) nm. IR (KBr) ν (cm^{-1}): 1600 cm^{-1} (CO_{str}, NH_{def}), ~2365–3680 cm^{-1} ($O\text{–}H_{str}$, signal of COOH H-bonding stabilized dimers), 1711 cm^{-1} (CO_{str}).

The formation of the NiOBCPPc-SWCNT-phenylamine hybrid is summarized as in Scheme 2. DCC, a popular coupling agent in organic synthesis, was used to facilitate the formation of amide bonds between the SWCNT-phenylamine and the NiOBCPPc in DMF. 20 mg (0.01 mmol) NiOBCPPc was dissolved in DMF and 32.85 mg (0.16 mmol) DCC was added in order to convert the COOH groups into active carbodiimide esters and was left in nitrogen

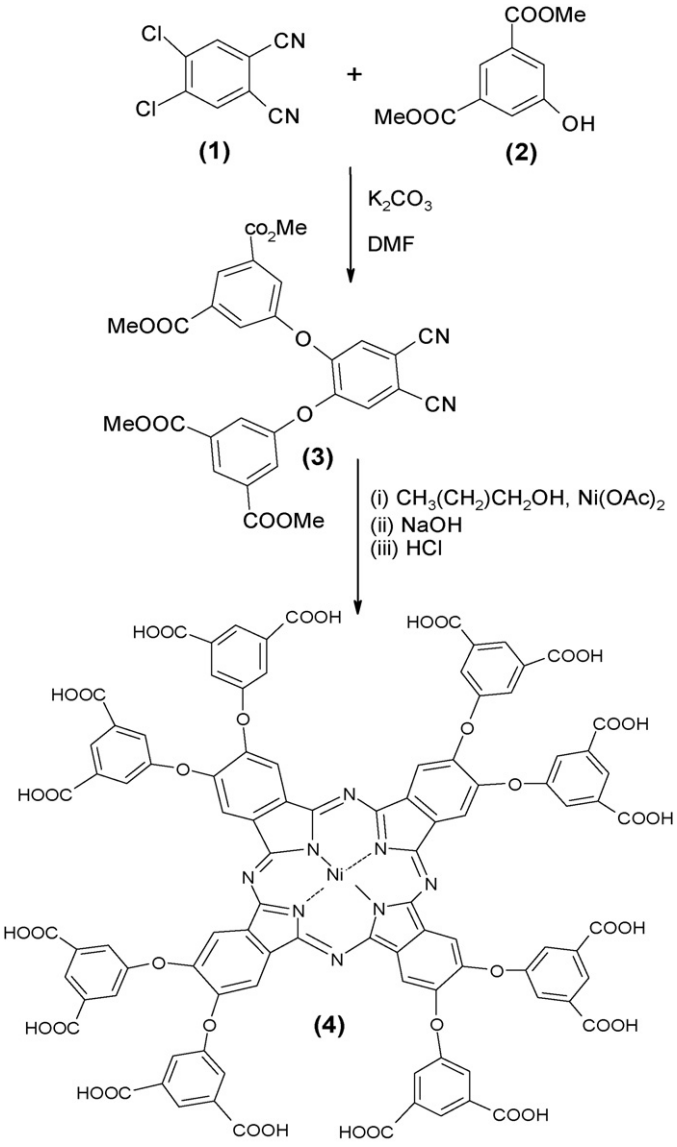

Scheme 1. Schematic of the synthesis route for NiOBCPPc.

atmosphere under stirring for 24 h at room temperature. Thereafter, 20 mg of SWCNT-phenylamine was added into the reaction mixture and then left for another 12 h.

In order to separate out the product, the reaction mixture was poured into methanol and the resultant dark precipitate was filtered off. The filtered impure product was then repeatedly washed with a mixture of chloroform and methanol (1:10 v/v ratio). The dark green product was extracted from the reaction mixture with chloroform in a separating funnel in order to separate the hybrid from unreacted SWCNT-phenylamine and NiOBCPPc. Chloroform was then removed *in vacuo* leaving behind the dark green solid product, which was further purified by thorough washing in methanol and THF. A dark green solid powder of NiOBCPPc-SWCNT-phenylamine hybrid was obtained after drying. IR (KBr) ν (cm^{-1}): NH_{str} (from amide bond) at 2923 cm^{-1}. λ_{max} (nm) ($\log\varepsilon$) in DMF: 266 nm (originated from CNT), the two broad Q-bands, aggregated and monomeric at ~636 and 678 nm.

2.2. Apparatus and procedure

High-resolution electron spray ionization Fourier transform ion cyclotron resonance (ESI-FTICR) mass spectra were measured with

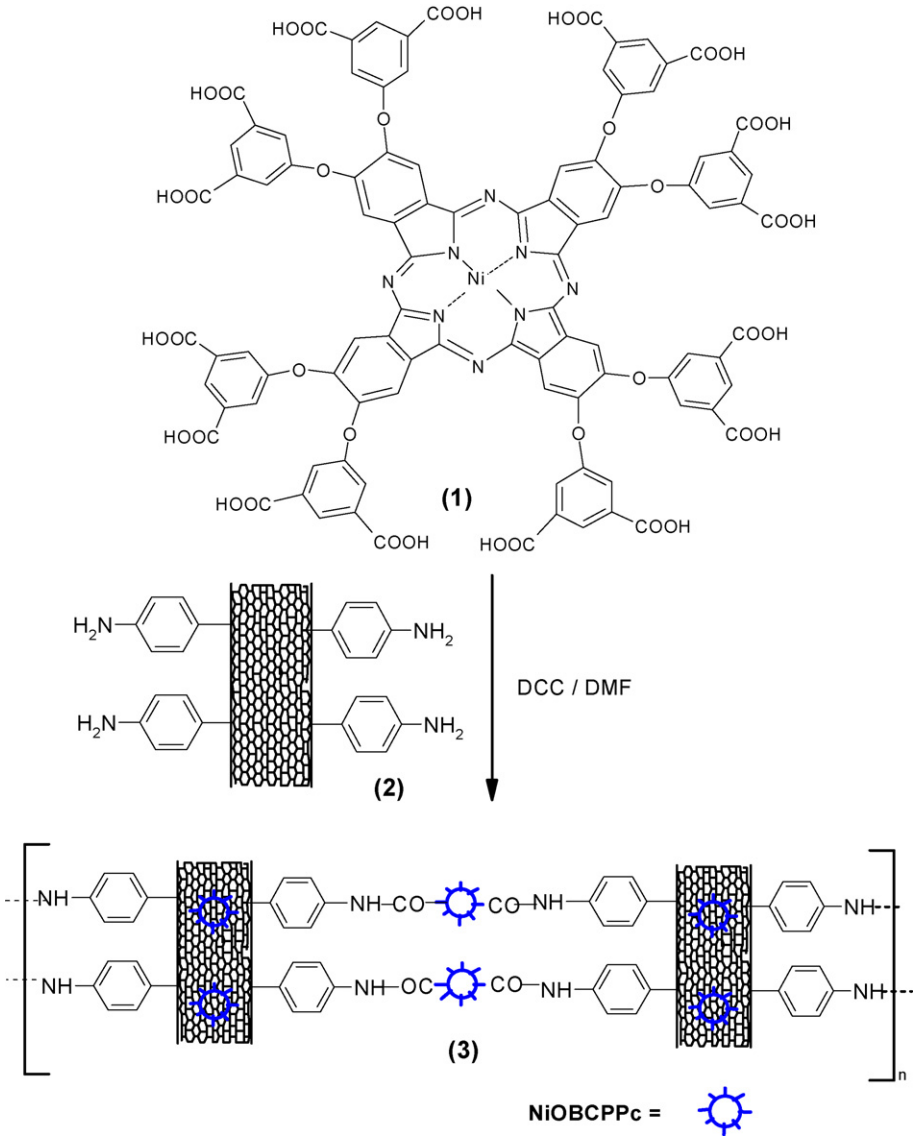

Scheme 2. Schematic of the synthesis route for NiOBCPPc-SWCNT-phenylamine hybrid.

a Bruker APEX III spectrometer by employing the negative ion mode. Elemental analysis of the synthesized NiOBCPPc complex was carried out using a Yanaco JM-10 CHN analyzer. Perkin-Elmer GX 2000 FTIR Spectrometer attached to a Perkin-Elmer Auto Image microscope system equipped with liquid nitrogen cooled MCT detector was used for IR analysis. Field emission scanning electron microscopy (FESEM) data were obtained using JEOL JSM 5800LV. Electrochemical studies were carried out using an Autolab potentiostat PGSTAT 302 (Eco Chemie, Utrecht, The Netherlands) driven by the General Purpose Electrochemical Systems data processing software (GPES, software version 4.9). The working electrode was glassy carbon electrode (GCE, BAS, $A = 0.0721\ cm^2$) modified with the SWCNTs or its NiOBCPPc hybrid. Ag|AgCl, sat'd KCl reference and platinum wire counter electrodes were employed. Electrochemical impedance spectroscopy (EIS) measurements were performed with Autolab FRA software between 10 kHz and 10 mHz using a 5 mV rms sinusoidal modulation. All experiments were performed at room temperature ($25 \pm 1\ ^\circ C$). Solutions were deaerated by bubbling nitrogen prior to the experiments and the electrochemical cells were kept under a nitrogen atmosphere throughout the experiments.

2.3. Electrode modification

The GCE surface was first cleaned by polishing with aqueous slurry of alumina followed by rinsing with distilled water, sonicated in ethanol and finally dried in gentle flow of nitrogen gas. The modification of the electrode by drop-dry method with materials (NiOBCPPc, SWCNT-phenylamine or NiOBCPPc-SWCNT-phenylamine hybrid) was then carried out. Briefly, 20 μL of the modifier solution (2 mg modifier in 1 mL dry DMF) was drop-cast onto the GCE surface and dried in oven at 50 °C for 1 h and allowed to cool to room temperature before use. A 1 M Na_2SO_4 electrolyte was used in all electrochemical measurements.

3. Results and discussion

A procedure for the synthesis of the zinc analogue reported in literature [47] was modified and used in this work for the synthesis of the NiOBCPPc analogue. Single-walled carbon nanotubes (SWCNTs) were converted to SWCNT-phenylamine using the established procedure reported in literature [46]. Scheme 2 shows the

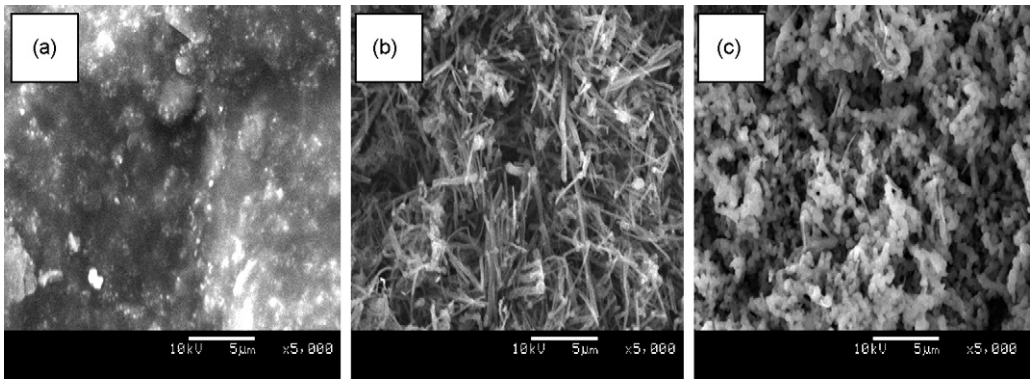

Fig. 1. SEM image of (a) NiOBCPPc, (b) SWCNT-phenylamine and (c) NiOBCPPc-SWCNT-phenylamine hybrid.

synthetic route employed for the synthesis of NiOBCPPc-SWCNT-phenylamine hybrid.

3.1. SEM characterization

Fig. 1 present comparative FESEM images of the NiOBCPPc (a), SWCNT-phenylamine (b) and NiOBCPPc-SWCNT-phenylamine hybrid (c) obtained on glassy carbon substrates.

Clearly, the NiOBCPPc-SWCNT-phenylamine hybrid displays a distinct image difference from those of the individual species, characteristic of a network of porous polymeric material, confirming the close association of the NiOBCPPc and SWCNT-phenylamine species via amide bond formation and some π–π interactions. SWCNTs are recognized as "the ultimate polymer" [48], thus the ability of the amino-functionalized SWCNTs to form a polymeric product with carboxy-functionalized NiPc complex using the synthesis strategy adopted in this work is very likely.

3.2. Spectroscopic (FTIR and UV–vis) characterization

The IR spectra overlays of (i) NiOBCPPc ("Na form"), (ii) NiOBCPPc, (iii) SWCNT-phenylamine and (iv) NiOBCPPc-SWCNT-phenylamine are shown in Fig. 2. The NiOBCPPc ("Na form") form of the complex showed the typical anti-symmetrical and symmetrical CO_{str} signals for carboxylate anion at 1565 and 1392 cm^{-1}, respectively. The signals obtained for NiOBCPPc confirmed the conversion of the COO^-Na^+ to the COOH group. The NiOBCPPc IR spectrum did not show the prominent COO^- dimers signal observed for NiOBCPPc ("Na form") but signals due to the COOH were clearly observed. The broad peaks that appeared in the ~2365–3680 cm^{-1} range is the $O–H_{str}$ signal of the COOH hydrogen-bonding stabilized dimmers, while that of the CO_{str} appear as single peak at 1711 cm^{-1}. The NH_{str} of the SWCNT amine appeared at 2915 cm^{-1} in SWCNT-phenylamine IR spectrum. The IR spectrum of the NiOBCPPc-SWCNT-phenylamine showed the NH_{str} at 2923 cm^{-1} and there is an absence of the COOH dimers broad signal (~2365–3680 cm^{-1}) confirming the conversion of COOH to amide bond. The overlapped peaks around 1600 cm^{-1} can be ascribed to mainly CO_{str} and NH_{def} of the amide bond of the NiOBCPPc-SWCNT-phenylamine. Indeed, it is interesting to observe that upon integration with the SWCNT-phenylamine, the –COOH broad band of the NiOBCPPc in the ~2365–3680 cm^{-1} region is replaced by a very sharp peak at 2923 cm^{-1} (ascribed to NH_{str}), indicative of the formation of the amide bond. Indeed, this amide bond NH_{str} is sharper than that of the amino group of the SWCNT-phenylamine that occurred at 2915 cm^{-1}; the full width at half maximum (FWHM) for the NH_{str} the NiOBCPPc-SWCNT-phenylamine is 40 cm^{-1}, while that of the SWCNT-phenylamine is approximately 10 cm^{-1}.

Electronic spectra (in the visible region; 500–900 nm) of (i) NiOBCPPc, (ii) SWCNT-phenylamine and (iii) NiOBCPPc-SWCNT-phenylamine hybrid in DMF are as shown in Fig. 3. The monomeric Q-band peak of NiOBCPPc is at 621 nm, while the complex also showed aggregated Q-band appearing at 667 nm. Aggregation in MPc complexes is typified by a broadened or split Q-band, with the

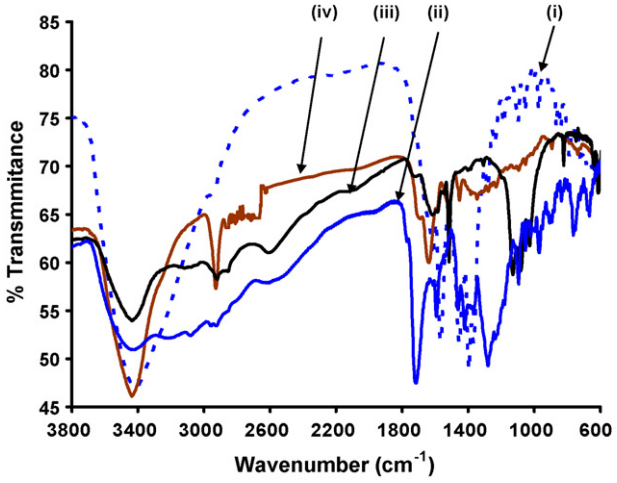

Fig. 2. FTIR spectra of ((i) NiOBCPPc ("Na form"), (ii) NiOBCPPc, (iii) SWCNT-phenylamine and (iv) NiOBCPPc-SWCNT-phenylamine hybrid.

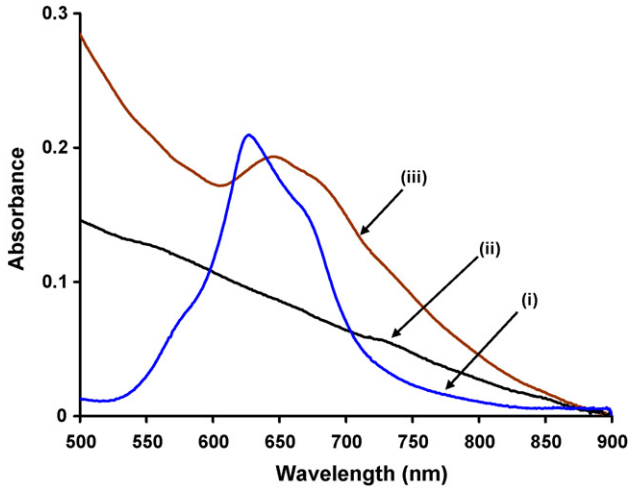

Fig. 3. Electronic spectra (in the visible region; 500–900 nm) of (i) NiOBCPPc, (ii) SWCNT-phenylamine and (iii) NiOBCPPc-SWCNT-phenylamine hybrid.

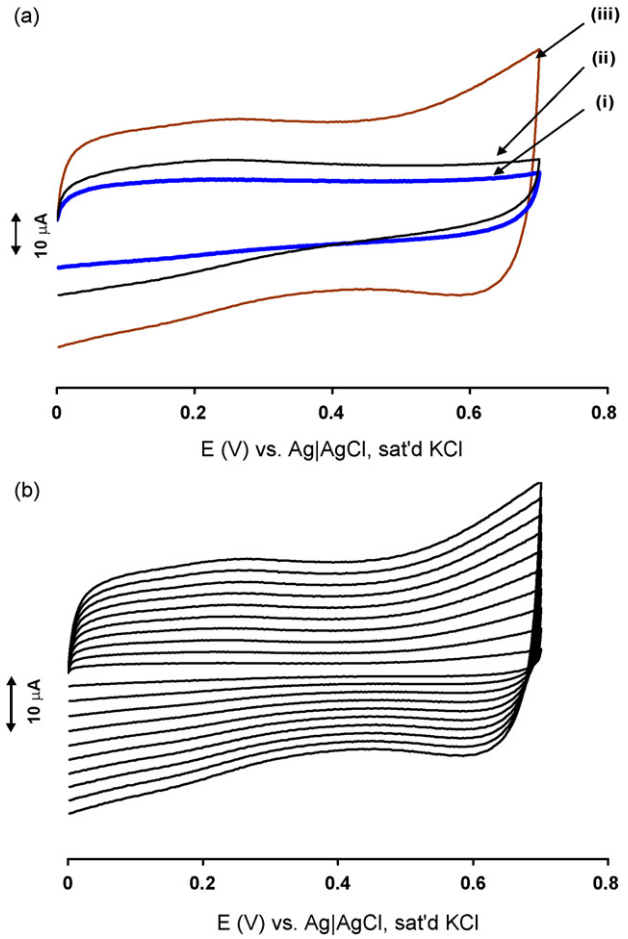

Fig. 4. (a) Cyclic voltammograms of (i) GCE-NiOBCPPc, (ii) SWCNT-phenylamine and (iii) NiOBCPPc-SWCNT-phenylamine hybrid in Na_2SO_4 aqueous solution at 0.1 V s^{-1} sweep rate and CVs pattern at different scan rate.

high energy band being due to the aggregate and the low energy band due to the monomer.

In the NiOBCPPc-SWCNT-phenylamine spectrum, the Q-band appears as one very broad aggregated form peak at ~650 nm; this also provides evidence the polymeric nature of the NiOBCPPc-SWCNT-phenylamine. The fact that the hybrid still exhibited the main electronic properties of NiOBCPPc means that the electronic structures of these two materials were not significantly altered on formation of the NiOBCPPc-SWCNT-phenylamine hybrid via non-covalent (π–π interaction) and via covalent (amide formation) between their functional groups. In summary, the spectroscopic data confirm the coupling of the two species (NiOBCPPc and SWCNT-phenylamine). This should be expected considering (i) the well-established ability of the DCC to couple phenylamines with carboxylic acid species [49], and (ii) that the amino group of the SWCNT-phenylamine is quite reactive [46]. In addition, given that SWCNTs are "the ultimate polymer" [48], the ability of the SWCNT-phenylamine to form a polymeric product with carboxy-functionalized NiPc complex using the synthesis strategy adopted in this work cannot be ruled out.

3.3. Cyclic voltammetry experiments

Fig. 4a shows the cyclic voltammograms obtained at sweep rates 0.1 V s^{-1} in 1 M Na_2SO_4 at (i) GCE-NiOBCPPc, (ii) GCE-SWCNT-phenylamine and (iii) GCE-NiOBCPPc-SWCNT-phenylamine hybrid.

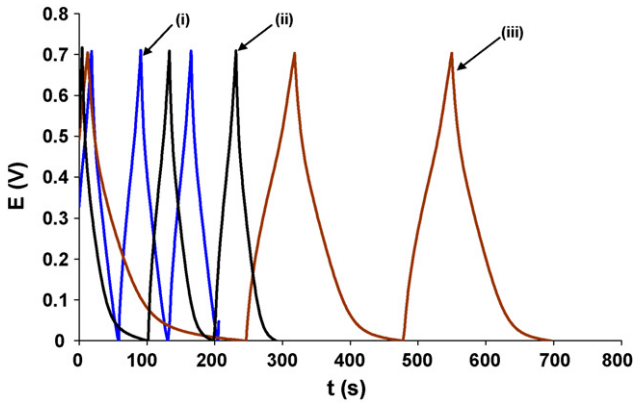

Fig. 5. Galvanostatic charge–discharge curve of (i) GCE-NiOBCPPc, (ii) SWCNT-phenylamine, and (iii) NiOBCPPc-SWCNT-phenylamine hybrid in 1 M Na_2SO_4 electrolyte. Applied current density = 138 μA cm^2.

It could be observed that the cyclic voltammograms (CVs) showed near rectangular-shape in the 0–0.4 V region with a weak redox process (anodic wave at ≈0.25 V and cathodic wave at ≈0.16 V, attributed to the Ni^{2+}/Ni^{3+}, generally known for its weak appearance [50]), and a redox couple in 0.4–0.6 V region (attributed to the first redox process of the phthalocyanine ring (Pc^{2-}/Pc^{3-}) [50]). The CVs clearly indicate the overall electrochemical process is a combination of double-layer capacitance (non-Faradaic) and pseudocapacitance (Faradaic) processes. Fig. 4b shows the CVs pattern at different scan rate for GCE-NiOBCPPc-SWCNT-phenylamine hybrid. Increasing scan rate, the CV pattern maintain their rectangular-shape but with increasing magnitude. These observations suggest that (i) the electrode is charged and discharge at pseudo-constant rate [51] and (ii) the diffusion of ion from the electrolyte into the pores is easily accessible irrespective of the potential sweep rate [52,53]. Similar trend (not shown) were also observed for GCE-NiOBCPPc and GCE-SWCNT-phenylamine, however, the order of the magnitude of the CVs at the same potential sweep rate decreases as follows; NiOBCPPc-SWCNT-phenylamine hybrid > SWCNT-phenylamine > NiOBCPPc, indicating capacitive behaviour in the same order. The capacitive behaviour is examined in detail using the more reliable galvanostatic charge–discharge strategy.

3.4. Galvanostatic charge–discharge

Galvanostatic discharge represents the most accurate and reliable strategy for probing the supercapacitance of materials. Fig. 5 shows the galvanostatic charge–discharge curves obtained for (i) GCE-NiOBCPPc, (ii) SWCNT-phenylamine and (iii) NiOBCPPc-SWCNT-phenylamine hybrid at a current density of 138 μA cm^{-2} in a 1 M Na_2SO_4 electrolyte. It could be observed that the shapes of the CD curves, irrespective of the material, are nearly symmetrical indicating good capacitive behaviour.

The specific capacitance (SC) was evaluated from the discharge curve using Eq. (1):

$$SC(F\,cm^{-2}) = \frac{I \times \Delta t}{\Delta E \times A} \quad (1)$$

where Δt is the discharge time in seconds, ΔE is the potential difference in volt, I is the applied current in ampere, A (cm^2) the area of the electrode.

The capacitance values, obtained at a current density of 138 μA cm^2, decrease as follows: NiOBCPPc-SWCNT-phenylamine (185.9 ± 0.6 mF cm^{-2}) > SWCNT-phenylamine (73.5 ± 0.7 mF cm^{-2}) > NiOBCPPc 54.1 ± 0.4 mF cm^{-2}). This trend is the same as for the CV data, except that higher values were obtained

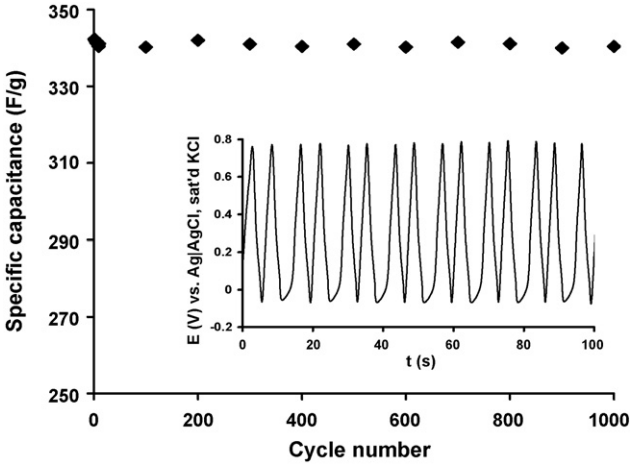

Fig. 6. Cyclic life of the NiOBCPPc-SWCNT-phenylamine hybrid in 1 M Na_2SO_4 aqueous electrolyte; the insets shows a section of the charge/discharge curves of the respective materials. Applied current density = 13.8 mA cm^2.

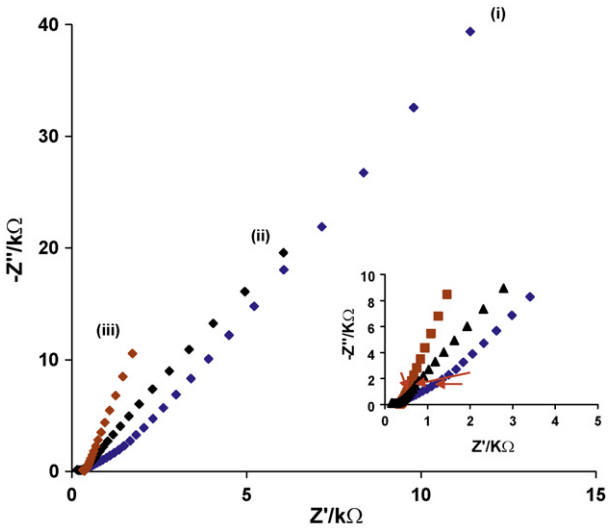

Fig. 7. Nyquist plots of (i) GCE-NiOBCPPc, (ii) SWCNT-phenylamine and (iii) NiOBCPPc-SWCNT-phenylamine hybrid in Na_2SO_4 aqueous solution at bias potential 0.4 V vs. Ag|AgCl, sat'd KCl. Inset is the scale-expanded high frequency sections.

from the CV data, the reason for which is not understood. However, the values from the galvanostatic discharge method are considered more reliable. The fact that the NiOBCPPc-SWCNT-phenylamine hybrid showed the highest value is an indication that its arrangement permits more suitable porosity for the ions to access and get inserted than both SWCNT-phenylamine and NiOBCPPc as separately entities. Other factors that could be responsible for the superior capacitive behaviour of the NiOBCPPc-SWCNT-phenylamine hybrid are (i) the high area support is provided by SWCNT-phenylamine for NiOBCPPc, and (ii) the charge inbalance which might be created by the attachment of already charged NiOBCPPc dispersed onto the SWCNT-phenylamine via π–π interaction in that way a "charge inbalance" is created which will provide more attachment of counter ions from the electrolyte solution to balance the charged surface and thus resulting to higher double-layer charging.

The energy deliverable efficiency (η/%) was obtained from Eq. (2).

$$\eta(\%) = \frac{t_d}{t_c} \times 100 \quad (2)$$

where t_d and t_c are discharge time and charging time, respectively. The energy deliverable efficiency for NiOBCPPc-SWCNT-phenylamine hybrid is 118.2 ± 1.1%. This implies that it takes longer time for the NiOBCPPc-SWCNT-phenylamine hybrid material to be discharged than the time it takes to charge it.

The long-term cycling stability of these materials as potential supercapacitor materials was investigated. Fig. 6 shows the cyclic life of the NiOBCPPc-SWCNT-phenylamine hybrid at a current density of 13.8 mA cm^2 in 1 M Na_2SO_4 electrolyte. The inset of the plot shows sections of the charge–discharge curves obtained at the GCE-NiOBCPPc-SWCNT-phenylamine hybrid electrode.

No significant differences in the capacitance were observed during the 1000 cycles except for initial decrease of about 5% in the first 10 cycles and thereafter no capacitance significant decreases were observed. This observation indicates that the NiOBCPPc-SWCNT-phenylamine hybrid has stability ability as a material for super capacitors and this could be due to their insignificant structural changes during the course of charge–discharge processes.

3.4.1. 3.5. Electrochemical impedance spectroscopy experiments

More insights into the electrochemical properties of these materials as related to their capacitive behaviour were carried out using EIS experiments in 1 M Na_2SO_4. Fig. 7 presents comparative Nyquist plots of (i) GCE-NiOBCPPc, (ii) SWCNT-phenylamine and (iii) GCE-NiOBCPPc-SWCNT-phenylamine hybrid in 1 M Na_2SO_4 aqueous solution at a bias potential of 0.4 V. EIS measurements carried out at several other potentials are not significantly different from that of 0.4 V.

The intercept at real part $-Z''$ (which is equivalent to the solution resistance, R_S) of the Nyquist plots of all the materials at very high frequencies are not significantly different from one another, this means that there are no significant differences in their summation of the various combination of resistances such as ionic resistance of electrolyte, intrinsic resistance of active materials, and contact resistance at the active material/electrode interface [54]. The points indicated by red arrows (Fig. 7 inset) are points which divide the high frequency component of the Nyquist plots from the low frequency component; these points are referred to as the knee frequency points [28,55]. The frequency at this point indicates the maximum frequency at which predominantly capacitive behaviour of these materials can be maintained [28]. The hybrid value was the highest with a high frequency of 142.5 Hz followed by that of SWCNT-phenylamine with 88.9 Hz and lastly NiOBCPPc (55.4 Hz). This trend indicates that the hybrid has a superior capacitive ability than the individual SWCNT-phenylamine and NiOBCPPc species. At the lower frequencies, a straight line (ideally 45° to the imaginary ($-Z''$) axis) represents the diffusive resistance (Warburg impendence, W) of the electrolyte and in this case the resistance of the diffusion of the electrolyte ions into the pores of these materials. Also, ideally for a pure capacitive behaviour the impedance should approach 90°, that is, vertical, and parallel to the imaginary ($-Z''$) axis [4]. The pattern observed for all the materials could be described as for a pseudocapacitive behaviour. The closer the "diffusion line" to the imaginary ($-Z''$) axis the lower the resistance to diffusion [29]. The order of closeness of the "diffusing line" for the materials is as follows: GCE-NiOBCPPc-SWCNT-phenylamine hybrid > SWCNT-phenylamine > NiOBCPPc. Once again, it can be implied from the observation that the hybrid material has a better porosity for the diffusion of the ions into its network. The observed experimental data could be modelled by the modified Randles equivalent circuit (Fig. 8) for all the three electrodes. In the circuit, R_s represent the solution resistance, R_{ct} represents the charge transfer resistance at the solution-electrode material film surface, CPE_1 and CPE_2 represent the constant phase elements which describe the roughness nature of the electrode surface [56] and the film capacitance respectively.

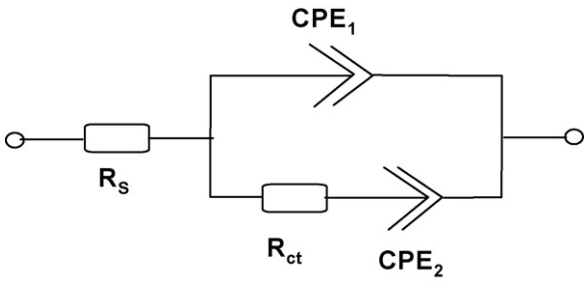

Fig. 8. Electrical equivalent circuit used in fitting the experimental EIS data obtained. Applied potential at 0.4 V vs. Ag|AgCl, sat'd KCl.

The most important parameter here is the R_{ct} whose value decreases as: NiOBCPPc (6.24 kΩ) > SWCNT-phenylamine (0.48 kΩ) > NiOBCPPc-SWCNT-phenylamine hybrid (0.24 kΩ), implying that the NiOBCPPc-SWCNT-phenylamine hybrid electrode has the least resistance to charge transfer.

Fig. 9 shows the plot of the imaginary impedance vs. $(2\pi f)^{-1}$ for (i) GCE-NiOBCPPc, (ii) GCE-SWCNT-phenylamine and (iii) GCE-NiOBCPPc-SWCNT-phenylamine hybrid generated from Fig. 5 data.

The inverse of the slope of this plot equals the low frequency capacitance, C_{lf} of these materials using Eq. (3) [28,57]:

$$C_{lf} = (2\pi f Z'')^{-1} \quad (3)$$

where C_{lf} is the low frequency capacitance (F), f is the frequency in (Hz) and Z'' is the imaginary impedance (Ω). The capacitance decreases as follows: NiOBCPPc-SWCNT-phenylamine (82.4 ± 0.7 mF cm^{-2}) > SWCNT-phenylamine (44.2 ± 0.5 mF cm^{-2}) > NiOBCPPc 22.2 ± 0.3 mF cm^{-2}). This trend is the same as obtained from the galvanostatic discharge, except that the values are lower than those from the galvanostatic method are higher. While the SC values of the SWCNT-phenylamine and NiOBCPPc are in the same magnitude as obtained from the galvanostatic experiment, the SC value of the NiOBCPPc-SWCNT-phenylamine hybrid obtained from the galvanostatic method is about a magnitude higher than obtained from the EIS. This is interesting considering that other workers [58] have observed that the value of SC obtained from galvanostatic experiment is about a magnitude greater than the value obtained for the same polymeric material from EIS experiment. The deviation of the SC from the EIS experiments from those determined from the galvanostatic experiments should perhaps not be surprising as

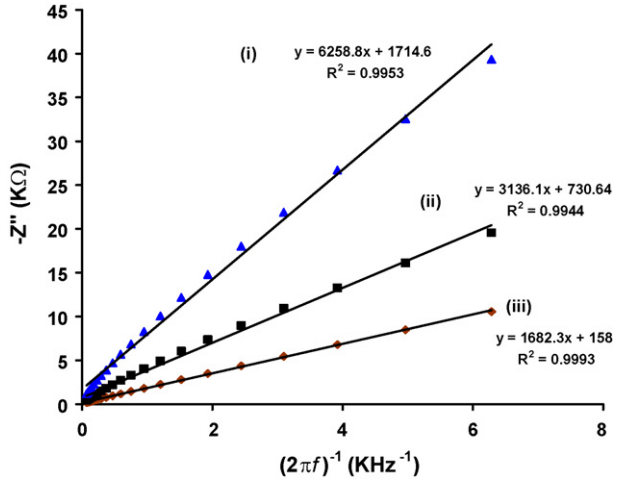

Fig. 9. Plot of the imaginary impedance vs. $(2\pi f)^{-1}$ generated from Fig. 5 data. (i) GCE-NiOBCPPc, (ii) SWCNT-phenylamine and (iii) NiOBCPPc-SWCNT-phenylamine hybrid.

previous workers [58–67] have also reported such deviation on conducting polymeric substances. Note that SWCNTs have also been regarded as the ultimate polymeric material [48]. The source of this deviation has been a subject of intense debate for more two decades. For example, Murray and co-workers [59] believed that source stems from the involvement of some physical and chemical heterogeneities; Tanguy et al. [61] ascribed it to some "deeply trapped" counter ions which remain immobile during impedance experiment; while other researchers have attributed this to the sluggish conformational changes occurring in the polymer network [56,57], "redox-switching hysteresis", [66] or the hindrance to the penetration of alternating current into the bulk electrode [67].

4. Conclusions

In conclusion, NiOBCPPc and its hybrid (NiOBCPPc-SWCNT-phenylamine) with SWCNT-phenylamine syntheses were successfully carried out as judged by the satisfactory characterization using various techniques such as IR, UV–vis spectroscopes. SEM images revealed the porous nature of NiOBCPPc-SWCNT-phenylamine hybrid when deposited on glassy carbon by drop-dry method. Cyclic voltammetry, galvanostatic charge–discharge cycling and impedimetric techniques all confirmed that NiOBCPPc-SWCNT-phenylamine hybrid has superior capacitive ability over NiOBCPPc and SWCNT-phenylamine judging by the higher values of specific capacitance obtained. The cyclic stability data shows that the three materials exhibited high stabilities with no significant changes over a cycling of 1000 times.

Acknowledgments

This work was supported by the NRF's "unlocking the future" programme (GUN # 2073666) and CSIR. BA also thanks NRF for Scarce Skill Postdoctoral Fellowship award that made this investigation possible.

References

[1] E. Frackowiak, F. Beguin, Carbon 39 (2001) 937.
[2] M. Endo, T. Maeda, T. Takeda, Y.J. Kim, K. Koshiba, H. Hara, M.S. Dresselhaus, J. Electrochem. Soc. 148 (2001) A910.
[3] P.L. Taberna, P. Simon, J.F. Fauvarque, J. Electrochem. Soc. 150 (2003) A292.
[4] B.E. Conway (Ed.), Electrochemical Supercapacitors: Scientific Fundamentals and Technological applications, Kluwer Academic/Plenum Press, New York, 1999.
[5] P. Bruce, B. Scrosati, J.M. Tarascon, W. van Schalkwijk, Nat. Mater. 4 (2005) 366.
[6] B.E. Conway, J. Electrochem. Soc. 138 (1991) 1539.
[7] C. Arbizzani, M. Mastragostino, B. Scosati, H.S. Nalwa (Eds.), Handbook of Organic Conductive Molecules and Polymers, vol. 4, Wiley, Chichester, UK, 1997, p. 595.
[8] A.F. Burke, T.C. Murphy (Eds.), Materials for Energy Storage and Conversion: Batteries, Capacitors and Fuel Cells, Materials Research Society, D.H. Goughtly, B. Vyas, T. Takamura, J.R. Huff, Pittsburgh, 1995, p. 375.
[9] S. Sarangapani, B.V. Tilak, C.P. Chen, J. Electrochem. Soc. 143 (1996) 3791.
[10] S.S. Fan, M.G. Chapline, N.R. Franklin, Science 283 (1999) 512.
[11] Z.W. Pan, S.S. Xie, L. Lu, Appl. Phys. Lett. 74 (1999) 3152.
[12] J.F. Silva, S. Griveau, C. Richard, J.H. Zagal, F. Bedioui, Electrochem. Commun. 9 (2007) 1629.
[13] J. Pillay, K.I. Ozoemena, Chem. Phys. Lett. 441 (2007) 72.
[14] J.R. Siqueira Jr., L.H.S. Gasparotto, F.N. Crespilho, A.J.F. Carvalho, V. Zucolotto, O.N. Oliveira, J. Phys. Chem. B 110 (2006) 22690.
[15] J.H. Zagal, S. Griveau, K.I. Ozoemena, T. Nyokong, F. Bedioui, J. Nanosci. Nanotechnol. 9 (2009) 2201.
[16] J.R. Siqueira Jr., F.N. Crespilho, V. Zucolotto, O.N. Oliveira Jr., Electrochem. Commun. 9 (2007) 2676.
[17] M. Siswana, K.I. Ozoemena, T. Nyokong, Electrochim. Acta 52 (2006) 114.
[18] B.O. Agboola, A. Mocheko, J. Pillay, K.I. Ozoemena, J. Porphyrins Phthalocyanines 12 (2008) 1289.
[19] B.O. Agboola, S.L. Vilakazi, K.I. Ozoemena, J. Solid State Electrochem. 13 (2009) 1367.
[20] G.T. Wu, C.S. Wang, X.B. Zhang, H.S. Yang, Z.F. Qi, P.M. He, W.Z. Li, J. Electrochem. Soc. 146 (1999) 1696.
[21] S.M. Lee, K.S. Park, Y.C. Choi, Y.S. Park, J.M. Bok, D.J. Bae, K.S. Nahm, Y.G. Choi, S.C. Yu, N.G. Kim, T. Frauennnheim, Y.H. Lee, Synth. Met. 113 (2000) 209.

[22] J.Y. Lee, K.H. An, J.K. Heo, Y.H. Lee, J. Phys. Chem. B 107 (2003) 8812.
[23] L. Diederich, E. Barborini, P. Piseri, A. Podesta, P. Milani, A. Schneuwly, R. Gallay, Appl. Phys. Lett. 75 (1999) 2662.
[24] K.H. An, W.S. Kim, Y.S. Park, Y.C. Choi, S.M. Lee, D.C. Chung, D.J. Bae, S.C. Lim, Y.H. Lee, Adv. Mater. 13 (2001) 497.
[25] V. Gupta, N. Miura, Electrochim. Acta 52 (2006) 1721.
[26] M. Deng, B. Yang, Z. Zhang, Y. Hu, J. Mater. Sci. 40 (2005) 1017.
[27] M. Deng, B. Yang, Y. Hu, J. Mater. Sci. 40 (2005) 5021.
[28] M. Hughes, G.Z. Chen, D.J. Fray, A.H. Windle, Chem. Mater. 14 (2002) 1610.
[29] A.L.M. Reddy, S. Ramaprabhu, J. Phys. Chem. C 111 (2007) 7727.
[30] B. Ballesteros, G. De la Torre, G.M.C. Ehli, A. Rahman, F. Agullo-Rueda, D.M. Guldi, J. Am. Chem. Soc. 129 (2007) 5061.
[31] H.-B. Xu, H.-Z. Chen, M.-M. Shi, R. Bai, M. Wang, Mater. Chem. Phys. 94 (2005) 342.
[32] Z.-L. Yang, H.-Z. Chen, L. Cao, H.-Y. Li, M. Wang, Mater. Sci. Eng., B 106 (2004) 73.
[33] G. Torre de la, W. Blau, T. Torres, Nanotechnology 14 (2003) 765.
[34] L. Cao, H. Chen, H.-B. Zhou, L. Zhu, J.-Z. Sun, X.-B. Zhang, J.-M. Xu, M. Wang, Adv. Mater. 15 (2003) 909.
[35] J.L. Bahr, J.M. Tour, J. Mater. Chem. 12 (2002) 1952.
[36] C.C. Leznoff, A.B.P. Lever, Phthalocyanines: Properties and Applications, vol.1–4, VCH publishers, New York, 1989–1996.
[37] K.I. Ozoemena, T. Nyokong, in: C.A. Grimes, E.C. Dickey, M.V. Pishko (Eds.), Encyclopedia of Sensors, vol. 3, American Scientific Publishers, California, 2006, pp. 157–200, chapter E.
[38] B.O. Agboola, K.I. Ozoemena, Phys. Chem. Chem. Phys. 10 (2008) 2399.
[39] B.O. Agboola, K.I. Ozoemena, Electroanalysis 20 (2008) 1696.
[40] F. Bedioui, S. Griveau, T. Nyokong, A.J. Appleby, C.A. Caro, M. Gulppi, G. Ochoa, J.H. Zagal, Phys. Chem. Chem. Phys. 9 (2007) 3383.
[41] K.I. Ozoemena, T. Nyokong, D. Nkosi, I. Chambrier, M.J. Cook, Electrochim. Acta 52 (2007) 4132.
[42] B. Agboola, P. Westbroek, K.I. Ozoemena, T. Nyokong, Electrochem. Commun. 9 (2007) 310.
[43] B.O. Agboola, K.I. Ozoemena, T. Nyokong, T. Fukuda, N. Kobayashi, Carbon (2009), doi:10.1016/j.carbon.2009.10.023.
[44] Y. Zhang, H. Feng, X. Wu, L. Wang, A. Zhang, T. Xia, H. Dong, X. Li, L. Zhang, Int. J. Hydrogen Energy 34 (2009) 4889.
[45] A.T. Chidembo, K.I. Ozoemena, B.O. Agboola, V. Gupta, G.G. Wildgoose and R.G. Compton, Energy Environ. Sci., 2009, doi:10.1039/b915920g.
[46] M.D. Ellison, P.J. Gasda, J. Phys. Chem. C 112 (2008) 738.
[47] W. Liu, T.J. Jensen, F.R. Fronczek, R.P. Hammer, K.M. Smith, M.G.H. Vicente, J. Med. Chem. 48 (2005) 1033.
[48] M. J. Green, N. Behabtu, M. Pasquali, W.W. Adams, Polymer 2009.(doi:10.1016/j.polymer.2009.07.044).
[49] J. Chen, S. Korner, S.L. Craig, S. Lin, D.M. Rudkevich, J. Rebek Jr., PNAS 99 (2002) 2593.
[50] A.B.P. Lever, E.L. Milaeva, G. Speier, in: C.C. Leznoff, A.B.P. Lever (Eds.), Phthalocyanines: Properties and Applications, vol. 3, VCH Publishers, New York, 1993, p. 1, Chapter 1.
[51] M. Xu, L. Kong, W. Zhou, H. Li, J. Phys. Chem. C 111 (2007) 19141.
[52] V. Gupta, T. Shinomiya, N. Miura, in: V. Gupta (Ed.), Recent Advances in Supercapacitors, Transworld Research Network, Kerala, India, 2006, pp. 17–28, chapter 2.
[53] M.W. Xu, D.D. Zhao, S.J. Bao, H.L. Li, J. Solid State Electrochem. 11 (2007) 1101.
[54] C.M. Niu, E.K. Sichel, R. Hoch, D. Moy, H. Tennent, Appl. Phys. Lett. 70 (1997) 1480.
[55] E. Barsoukov, J.R. Macdonald (Eds.), Impedance Spectroscopy: Theory Experiment and Applications, second edn., Wiley, Hoboken, NJ, 2005, Chapters 1–4.
[56] F. Fusalba, N. Elmehdi, L. Breau, D. Belanger, Chem. Mater. 11 (1999) 2743.
[57] X.W. Sun, X. Chen, J. Power Sources 193 (2009) 924.
[58] B.J. Feldman, P. Burgmayer, R.W. Murray, J. Am. Chem. Soc. 107 (1985) 872.
[59] N. Mermilliod, J. Tanguy, F. Petior, J. Electrochem. Soc. 133 (1986) 1073.
[60] J. Tanguy, N. Mermilliuod, M. Hoclet, J. Electrochem. Soc. 134 (1987) 795.
[61] T. Tanguy, M. Slama, M. Hoclet, J.L. Baudin, Synth. Met. 28 (1989) C145.
[62] M. Kalaji, L.M. Peter, J. Chem. Soc., Faraday Trans. 87 (1991) 853.
[63] X. Ren, P.G. Pickup, J. Electroanal. Chem. 372 (1994) 289.
[64] T.C. Girija, M.V. Sangaranarayanan, J. Appl. Electrochem. 36 (2006) 531.
[65] G. Xu, W. Wang, X. Qu, Y. Yin, L. Chu, B. He, H. Wu, J. Fang, Y. Bao, L. Liang, Eur. Polym. J. (2009), doi:10.1016/j.europolymj.2009.05.016.
[66] C. Du, N. Pan, J. Power Sources 160 (2006) 1487.
[67] W. Sun, X. Chen, J. Power Sources 193 (2009) 924.